Adsorption on surfaces

Example: H_2/H/Pd(210)

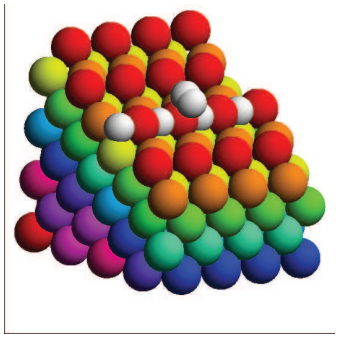

Adsorption of molecular and atomic hydrogen on Pd(210)

Theoretical description

Adsorption of molecules on surfaces technologically of tremendous importance

Theoretical description by *ab initio* methods possible

Analysis of electronic structure very useful for understanding of chemical trends

Approximate model Hamiltonian can provide qualitative insight: Newns-Anderson, Effective-Medium-Theory, Embedded-Atom-Method . . .

Bonding at surfaces

Lennard-Jones picture of dissociative adsorption

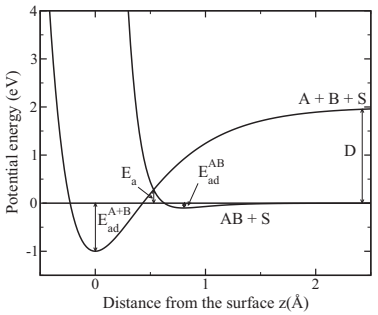

Potential energy curves for molecular and dissociative adsorption

Nature of surface bonds

Physisorption ($E_{ad} \lesssim 0.1$ eV): Noble gas adsorption, molecular adsorption through Van-der-Waals interaction

Chemisorption ($E_{ad} \sim 1$ - 10 eV): Chemical bond between surface and adsorbate

Nature of surface chemical bonds:

Metallic bonding

Alkali-metal bond (mainly ionic)

Covalent bonds

Potential energy surfaces (PES)

PES central quantity to describe gas-surface interaction; Example: catalyst

1D representation

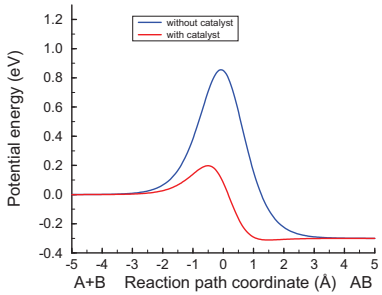

Multidimensional representation

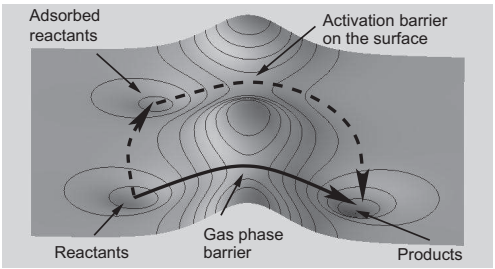

A. Groß, Surf. Sci. Vol. 500

1D representation misleading:

Catalysts provides detour in multi-dimensional configuration space with lower activation barriers

Physisorption

Physisorption mediated by Van der Waals forces

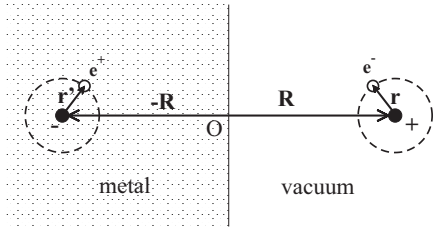

$\vec{R} = (0, 0, Z)$

$\vec{r} = (x, y, z)$

Image potential of a hydrogen atom in front of a metal surface:

$$V_{\rm im} = -\frac{e^2}{2}\left[\frac{1}{|2\vec{R}|} + \frac{1}{|2\vec{R}+\vec{r}+\vec{r}'|} - \frac{1}{|2\vec{R}+\vec{r}|} - \frac{1}{|2\vec{R}+\vec{r}'|}\right]$$
$$= -\frac{e^2}{2}\left[\frac{1}{2Z} + \frac{1}{2(Z+z)} - \frac{2}{|2\vec{R}+\vec{r}|}\right] . \qquad (103)$$

van der Waals interaction

Taylor expansion of image force in $|\vec{r}|/|\vec{R}|$:

$$V_{\rm im} = -\frac{e^2}{8Z^3}\left[\frac{x^2+y^2}{2} + z^2\right] + \frac{3e^2}{16Z^4}\left[\frac{z}{2}(x^2+y^2) + z^3\right] + \dots . \quad (104)$$

van der Waals interaction $\propto Z^{-3}$

Assumption: electronic motion in atom can be modeled by 3D-oscillator:

$$V_{\rm atom} = \frac{m_e\omega_{\rm vib}^2}{2}\left(x^2+y^2+z^2\right) . \quad (105)$$

Atom potential in the presence of the surface:

$$\begin{aligned} V_{\rm atom} &= \frac{m_e\omega_{\rm vib}^2}{2}\left(x^2+y^2+z^2\right) - \frac{e^2}{8Z^3}\left[\frac{x^2+y^2}{2} + z^2\right] + \dots \\ &\approx \frac{m_e\omega_\parallel^2}{2}\left(x^2+y^2\right) + \frac{m_e\omega_\perp^2}{2}z^2 . \end{aligned} \quad (106)$$

van der Waals interaction energy

Frequency of the atomic oscillator

$$V_{\rm atom} = \frac{m_e\omega_\parallel^2}{2}\left(x^2+y^2\right) + \frac{m_e\omega_\perp^2}{2}z^2 . \quad (107)$$

with

$$\omega_\parallel = \omega_{\rm vib} - \frac{e^2}{8m_e\omega_{\rm vib}Z^3} \text{ and } \omega_\perp = \omega_{\rm vib} - \frac{e^2}{4m_e\omega_{\rm vib}Z^3} . \quad (108)$$

van der Waals binding energy: change in zero-point energy of atomic oscillator

$$E_{vdW}(Z) = \frac{\hbar}{2}(\omega_\perp + 2\omega_\parallel - 3\omega_{\rm vib}) = \frac{-\hbar e^2}{4m_e\omega_{\rm vib}Z^3} . \quad (109)$$

van der Waals constant

Atomic polarizability

$$\alpha = \frac{e^2}{m_e\omega_{\rm vib}^2} . \quad (110)$$

van der Waals binding energy:

$$E_{vdW}(Z) = -\frac{\hbar\omega_{\rm vib}\alpha}{8Z^3} = -\frac{C_v}{Z^3} \quad (111)$$

$C_v = \hbar\omega_{\rm vib}\alpha/8$ van der Waals constant, related to the atomic polarizability

Fourth-order correction defines dynamical image plane at Z_0

$$V_{\rm im}(Z) = -\frac{C_v}{Z^3} - \frac{3C_vZ_0}{Z^4} + O(Z^{-5}) = -\frac{C_v}{(Z-Z_0)^3} + O(Z^{-5}) \quad (112)$$

Zaremba-Kohn picture of physisorption

Taylor expansion of image force of the hydrogen atom corresponds basically to dipole-dipole interaction at distance $2Z$

However, hydrogen atom in the ground state has no permanent dipole moment $\Rightarrow$ quantum treatment neccessary

Quantum derivation of the long-range interaction between a neutral atom and a solid surface (Zaremba, Kohn)

$$H = H_a + H_s + V_{as} . \quad (113)$$

a atom, s solid, V_{as} interaction term:

$$V_{as} = \int d^3\vec{r}d^3\vec{r}' \frac{\hat{\rho}^s(\vec{r})\hat{\rho}^a(\vec{r}')}{|\vec{r}-\vec{r}'|} \text{ with } \hat{\rho}^{s,a}(\vec{r}) = n_+^{s,a}(\vec{r}) - \hat{n}^{s,a}(\vec{r}) . \quad (114)$$

Pertubation treatment of physisorption

$$H = H_a + H_s + V_{as} \,. \tag{115}$$

First-order contribution vanishes; second order:

$$\begin{aligned} E^{(2)} &= \sum_{\alpha\neq 0}\sum_{\beta\neq 0} \frac{|\langle\psi_0^a\psi_0^s|V'_{as}|\psi_\alpha^a\psi_\beta^s\rangle|}{(E_0^a - E_\alpha^a) + (E_0^s - E_\beta^s)} \\ &= -\int d^3\vec{r}\int d^3\vec{r}'\int d^3\vec{x}\int d^3\vec{x}' \frac{1}{|\vec{R}+\vec{x}-\vec{r}|}\,\frac{1}{|\vec{R}+\vec{x}'-\vec{r}'|} \\ &\quad\times\int_0^\infty \frac{d\omega}{2\pi}\,\chi_a(\vec{x},\vec{x}',i\omega)\chi_s(\vec{r},\vec{r}',i\omega) \end{aligned} \tag{116}$$

$\chi_{a,s}$ retarded response functions

Pertubation treatment of physisorption II

Assumption: negligible overlap of the wave functions $\Rightarrow$

$$E^{(2)}(Z) = -\frac{C_v}{(Z-Z_0)^3} + O(Z^{-5}) \tag{117}$$

with

$$C_v = \frac{1}{4\pi}\int_0^\infty d\omega\;\alpha(i\omega)\,\frac{\epsilon(i\omega)-1}{\epsilon(i\omega)+1} \tag{118}$$

$$Z_0 = \frac{1}{4\pi C_v}\int_0^\infty d\omega\;\alpha(i\omega)\,\frac{\epsilon(i\omega)-1}{\epsilon(i\omega)+1}\,\bar{z}(i\omega) \tag{119}$$

α atomic polarizability, ϵ dielectric function, $\bar{z}$ centroid of induced charge density

Physisorption potential for He on noble metals

Physisorption potential

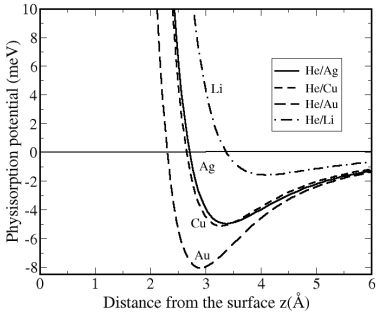

Potential as a function of Z

Theoretical description

Zaremba and Kohn, PRB 15, 1769 (1977): Interaction potential divided in two parts:

Short-range Hartree-Fock term

Longe-range van der Waals interaction

$$V(Z) = V_{\rm HF}(Z) + V_{\rm vdW}(Z) \tag{120}$$

Noble gas: repulsive interaction proporptional to surface charge density

$$V_{\rm HF}(Z) \propto n(Z) \tag{121}$$

van der Waals interaction in DFT

Localized electron hole in current exchange-correlation functionals
$\Rightarrow v_{eff}(z) \propto e^{-\alpha z}$ for $z\to\infty$ instead of $v_{eff}(z)\to 1/z$

Hult *et al.*: Adiabatic connection formula:

$$E_{xc}[n] = \frac{1}{2}\int d^3\vec{r}d^3\vec{r}'\frac{e^2}{|\vec{r}-\vec{r}'|}\int_0^1 d\lambda[\langle\tilde{n}(\vec{r})\tilde{n}(\vec{r}')\rangle_{n,\lambda} - \delta(\vec{r}-\vec{r}')\langle(\vec{r})\rangle] \tag{122}$$

$\Rightarrow$ Second order

$$\begin{aligned} \Delta E_{xc}(\vec{R}) &= E_{xc}^\infty - \int d^3\vec{r}\int d^3\vec{r}'\int d^3\vec{x}\int d^3\vec{x}' V_{as}(\vec{R}+\vec{x}-\vec{r})\;V_{as}(\vec{R}+\vec{x}'-\vec{r}') \\ &\quad\times\int_0^\infty \frac{d\omega}{2\pi}\,\chi_a(\vec{x},\vec{x}',i\omega)\chi_s(\vec{r},\vec{r}',i\omega) \end{aligned} \tag{123}$$

Approximations: Response treated in Random Phase Approximation (RPA)
local approximation for screened response

Chemisorption

Chemisorption corresponds to the creation of a true chemical bond between adsorbate and substrate

Energetic contributions to chemisorption discussed within DFT:

$$\begin{aligned} E_{\rm tot} &= \sum_{i=1}^{N} \varepsilon_i + E_{\rm xc}[n] - \int v_{\rm xc}(\vec{r}) n(\vec{r})\, d\vec{r} - E_{\rm H} + V_{\rm nucl-nucl} \\ &= \sum_{i=1}^{N} \varepsilon_i + E_{\rm xc}[n] - \int v_{\rm eff}(\vec{r}) n(\vec{r})\, d\vec{r} + E_{\rm H} + V_{\rm el-nucl} + V_{\rm nucl-nucl} \\ &= \sum_{i=1}^{N} \varepsilon_i + E_{\rm xc}[n] - \int v_{\rm eff}(\vec{r}) n(\vec{r})\, d\vec{r} + E_{\rm es} \end{aligned} \tag{124}$$

Newns-Anderson Model

Developed by Newns based on a model proposed by Anderson for bulk impurities

Describes the interaction of a adatom orbital ϕ_a with metal states ϕ_k

Model Hamiltonian (ignoring spin)

$$H = \varepsilon_a\, n_a + \sum_k \varepsilon_k\, n_k + \sum_k (V_{ak}\, b_a^+ b_k + V_{ka}\, b_k^+ b_a) \tag{125}$$

$$n_i = b_i^+ b_i \qquad i = a, k\,. \tag{126}$$

n_i number operator, b_i^+, b_i creation and annihilation operator of the orbital ϕ_i, respectively.

Adsorbate LDOS in the Newns-Anderson Model

Direct solution of the Schrödinger equation

$$H\, \vec{c}_i = \varepsilon_i\, \vec{c}_i \tag{127}$$

intractable due to the infinite number of metal states

Consider local density of states (LDOS) on the adsorbate level:

$$\rho_a(\varepsilon) = \sum_i |\langle i|a\rangle|^2\, \delta(\varepsilon - \varepsilon_i) = -\frac{1}{\pi}\, {\rm Im} G_{aa}(\varepsilon) \tag{128}$$

G single particle Green function ($\delta = 0^+$):

$$G(\varepsilon) = \sum_i \frac{|i\rangle\langle i|}{\varepsilon - \varepsilon_i + i\delta} \tag{129}$$

Adsorbate level in the Newns-Anderson Model

Single-particle Green function

$$G_{aa}(\varepsilon) = \frac{1}{\varepsilon - \varepsilon_a - \Sigma(\varepsilon)} \tag{130}$$

Self-energy $\Sigma(\varepsilon) = \Lambda(\varepsilon) - i\Delta(\varepsilon)$:

$$\Delta(\varepsilon) = \pi \sum_k |V_{ak}|^2\, \delta(\varepsilon - \varepsilon_k) \tag{131}$$

$$\Lambda(\varepsilon) = \frac{P}{\pi} \int \frac{\Delta(\varepsilon')}{\varepsilon - \varepsilon'} d\varepsilon'\,, \tag{132}$$

P denotes principal part integral

Parameters in the Newns-Anderson Model

Adsorbate LDOS:

$$\rho_a(\varepsilon) \;=\; \frac{1}{\pi}\,\frac{\Delta(\varepsilon)}{(\varepsilon-\varepsilon_a-\Lambda(\varepsilon))^2 \;+\; \Delta^2(\varepsilon)}\,. \qquad (133)$$

$\Delta(\varepsilon)$ lifetime broadening

Position of affinity level $\varepsilon_a(z)+\Lambda(z)$ and level width $\Delta(z)$ usually enter as parameters in the Newns-Anderson model

Newns-Anderson model rather for explanatory purposes than for predictive purposes helpful

Recently Newns-Anderson model predominantly used to describe charge transfer processes in molecule-surface scattering

Variation of adsorbate levels

Ionization energy and affinity level

Ionization energy I: energy to remove an electron from a neutral atom and bring it to infinity

Electron affinity A: energy that is gained when an electron is taken from infinity to the valence level of an atom

I and A modified in front of a surface:
Let us consider a hydrogen atom in front of a perfect conductor

$$V_{\rm im} = -\frac{e^2}{2}\left[\frac{1}{2Z}+\frac{1}{2z}-\frac{2}{(Z+z)}\right] \qquad (134)$$

I: attraction of electron to its own image charge overcompensated by repulsion with respect to the image of the nucleus

$$\Delta I = \int_{z=Z}^{\infty}\frac{\partial V_{\rm im}}{\partial z'}\,dz' \;=\; -\frac{e^2}{4z}\,. \qquad (135)$$

Level variation

A: Gain additional energy due to the interaction of the electron with its own image:

$$A_{\rm eff}(z) \;=\; A \;+\; \frac{e^2}{4z}\,. \qquad (136)$$

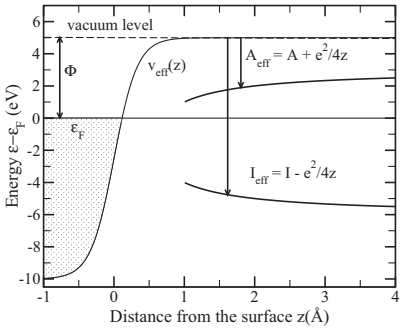

Occupied levels increase and affinity levels decrease in front of a surface

Adsorbate affinity level variation

Schematic picture

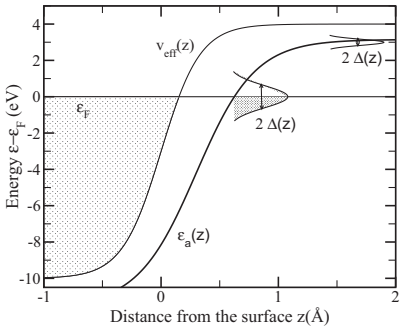

Variation of affinity level $\varepsilon_a(z)$

Theoretical description

Initially empty affinity levels shifts down:

$$\varepsilon_a(z) \;=\; \varepsilon_\infty \;-\frac{e}{4z} \qquad (137)$$

Width of the level increases:

$$\Delta(z) \;=\; \Delta_0\; e^{-\alpha z} \qquad (138)$$

When $\varepsilon_a(z)$ crosses the Fermi level, the level becomes filled

Close to the surface adsorbate is then negatively charged

Effective medium theory

Idea: Adsorbate can be considered as being embedded in an inhomogeneous electron gas set up by the substrate

Determine average electron density in the vicinity of the adsorbate

$$\bar{n}_i \;=\; <\sum_{j\neq i} n_j(\vec{r}) > \qquad (139)$$

Energy estimated as the embedding *cohesive* energy of the adsorbate in a homogeneous electron gas, the **effective** medium:

$$E \;\approx\; E_{ci}(\bar{n}_i) \qquad (140)$$

Cohesive energy $E_c(\bar{n})$ universal function

Embedding cohesive energies

Cohesive energies

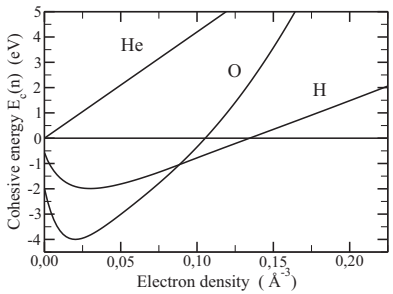

Embedding energy for H,O and He obtained by LDA-DFT
(M.J. Puska *et al.*, PRB 24, 3037 (1981))

Discussion

Two contributions to E_c: kinetic and electrostatic energy

Kinetic energy: increases with density due to the Pauli principle

Electrostatic energy: becomes more attractive at higher densities

Competition of kinetic and electrostatic energy leads to a minimum (except for noble gases)

$n \to 0$: $E_c \to A$: electron affinity

Qualitative picture of hydrogen adsorption

Hydrogen embedding energy as a function of the electron density

Electron density and potential variation

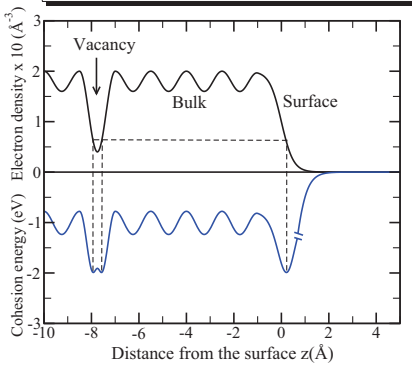

Energetics

Dashed line: Optimum density

Chemisorption minimum direct reflection of the minimum of the $E_c(n)$ curve

Hydrogen sits off-center in the vacancy since the electron density is to low in the center of the vacancy

Qualitative explanations given by embedding energy

Chemisorption bond length:
adsorbate-metal bond lengths are the shorter, the lower the adsorbate coordination is

Adsorbate-metal vibrational frequency:

$$\omega_{\rm vib} \propto \sqrt{\frac{d^2E_c(n(\vec{r}))}{dz^2}} = \sqrt{\frac{d^2E_c(n)}{dn^2}}\,\frac{dn}{dz} \tag{141}$$

Assumption: $n_{\rm atom} \propto \exp(-\beta r) \Rightarrow$

$$\frac{dn}{dz} = \beta\, n_0 \sin\alpha \tag{142}$$

α: angle of the metal-adsorbate line with the surface plane

$\Rightarrow \omega_{\rm vib}^{\rm top} > \omega_{\rm vib}^{\rm bridge} > \omega_{\rm vib}^{(111)\rm hollow} > \omega_{\rm vib}^{(100)\rm hollow}$

Effective medium theory II

Problems associated with simple form $E_{\rm tot} = E_c(n)$:

Adsorption energy independent of substrate

No diffusion barrier on the surface

$\Rightarrow$ Electrostatic interaction of the cores and band-structure effects have to be taken into acccount:

$$E_{\rm tot} = E_c(\bar{n}_0) + \int_a \phi_0(\vec{r})\Delta\rho(\vec{r})d^3(\vec{r}) + \delta\left(\int_{-\infty}^{\varepsilon_F}\Delta g(\varepsilon)\,\varepsilon\,d\varepsilon\right) \tag{143}$$

Final result:

$$E_{\rm tot} = E_c^{\rm eff}(\bar{n}_0) + \Delta E_{\rm hyb} \tag{144}$$

$$\Delta E_{\rm hyb} = -2\,(1-f)\,\frac{|V_{ad}|^2}{C_d - V_0(\vec{r})} \tag{145}$$

EMT adsorption energies on 3d and 4d metals

3d metals

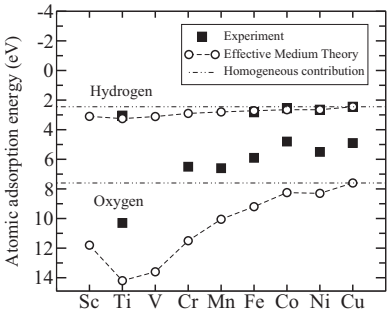

4d metals

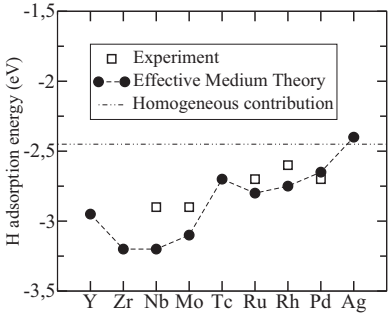

For atomic oxygen adsorption, the deviations between experiment and theory are already much larger ($\sim$ 2 eV)

Embedded Atom Method (EAM)

Idea (Daw and Baskes (1983)): Total energy is a sum of an embedding energy plus an electrostatic core-core repulsion

$$E_{\rm tot} \;=\; \sum_i F_i(n_{h,i}) \;+\; \frac{1}{2}\sum_{i\neq j} \phi_{ij}(r_{ij}) \tag{146}$$

$n_{h,i}$: host density at atom i due to the remaining atoms of the system
$\phi_{ij}(r_{ij})$: core-core pair repulsion between atoms i and j separated by r_{ij}

$n_{h,i}$ estimated as superposition of atomic densities

$$n_{h,i} \;=\; \sum_{j(\neq i)} n_j^a(r_{ij}) \tag{147}$$

$\phi_{ij}(r)$ represented by interaction of two neutral, screened atoms

$$\phi_{ij}(r) \;=\; Z_i(r)\; Z_j(r)\; /r\;. \tag{148}$$

Embedding energy and effective charge in the EAM

Embedding energy $F(n)$ and effective charge $Z(r)$ fitted to reproduce lattice and elastic constants, cohesive and vacancy formation energy, and energy difference between fcc and bcc phases.

Embedding energy

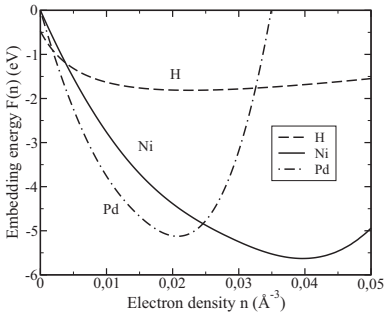

Effective charge

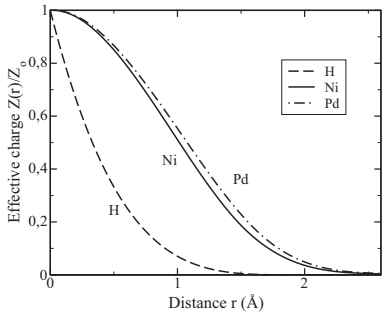

Hydrogen atomic chemisorption energies

Embedding energy $F(n)$ and effective charge $Z(r)$ fitted to reproduce lattice and elastic constants, cohesive and vacancy formation energy, and energy difference between fcc and bcc phases.

Method	Pd(100)			Pd(111)			
	hollow	bridge	top	fcc hollow	hcp hollow	bridge	top
EAM	0.53	0.45	0.10	0.53	0.53	–	0.03
GGA-DFT	0.468	0.426	-0.047	0.554	0.518	0.410	0.010

GGA-DFT results for 2×2 structure with the PW91-GGA functional (courtesy of A. Roudgar)

EAM gives reasonable description of hydrogen chemisorption energies

EAM used extensively for bulk and surface properties of metals and alloys

Covalent bonding

EMT and EAM give reasonable description of metal bonding and atomic chemisorption

EMT and EAM do not satisfactorily describe covalent bonding

EDIM method (Embedded diatomics in molecules; Truong, Truhlar):
EAM combined with semiempirical bond theory

EDIM: Expresses Coulomb and exchange integral in modified four-body LEPS form plus embedded atom ideas

Lang-Williams Theory of Atomic Chemisorption

Interaction of adsorbates with sp bonded metals (Al,Na):

DFT-LDA calculations of atomic adsorption on jellium surfaces

Theory of Atomic Chemisorption on Simple Metals, PRB **18**, 616 (1978).

Solution of Kohn-Sham equations can be regarded as being equivalent to solving a scattering Lippmann-Schwinger equation:

$$\psi_{MA}(\vec{r}) \;=\; \psi_M(\vec{r}) \;+\; \int d^3\vec{r}'\; G_M(\vec{r},\vec{r}')\; \delta v_{\rm eff}(\vec{r}')\; \psi_{MA}(\vec{r}') \qquad (149)$$

M: unperturbed metal; MA: metal-adsorbate system

$\delta v_{\rm eff}(\vec{r})$: Change of the effective potential due to the presence of the adsorbate

Interpretation: elastic scattering of metal states $\psi_M(\vec{r})$ by the adsorbate induced effective potential $\delta v_{\rm eff}(\vec{r})$

$\Rightarrow$ Charge density and local density of states in atomic chemisorption

Charge density in atomic chemisorption

Charge density plots

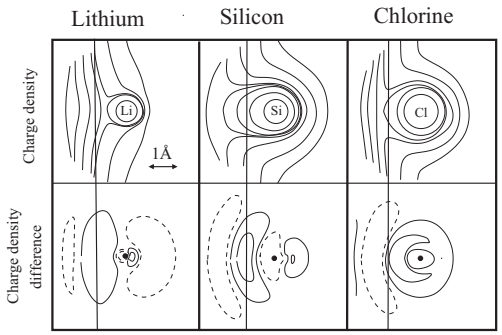

Upper panel: Total charge density of states; lower panel: charge density difference, broken lines correspond to charge depletion (Lang and Williams).

Charge density plots alone are often not very instructive

$\Rightarrow$ Charge density difference plot:

$$\Delta n(\mathbf{r}) = n(\mathbf{r})_{\rm total} - n(\mathbf{r})_{\rm substrate} - n(\mathbf{r})_{\rm atom} \qquad (150)$$

Type of chemisorption

Lithium:
charge transfer to substrate
$\Rightarrow$ positive ionic chemisorption

Chlorine
charge transfer to adsorbate
$\Rightarrow$ negative ionic chemisorption

Silicon
charge accumulation in bond region
$\Rightarrow$ covalent bonding

Spatial information about charge redistribution supplemented by analysis of the density of states:
$\Rightarrow$ Energetics corresponds to a balance between band-structure and electrostatic contributions

Change of the density of states upon adsorption

Density of states

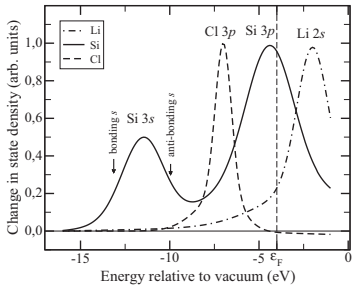

Change of the density of states (Lang and Williams). Electron density corresponds to Al ($r_s = 2$).

Type of chemisorption

Li $2s$ derived state primarily above ε_F
$\Rightarrow$ positive ionic chemisorption

Cl $3p$ derived state primarily below ε_F
$\Rightarrow$ negative ionic chemisorption

Si $3p$ derived state half-filled
$\Rightarrow$ covalent bonding

Charge contour plots:

Lower parts of the resonances add charge to the bond region, upper parts substract charge from this region
$\Rightarrow$ bonding – anti-bonding character

Bonding character of resonances

Lang and Williams: Bonding – anti-bonding character of resonances derived from charge contour plots

Alternative derivation: Phase shift of scattering states

$$\tan\delta_\alpha(\varepsilon) \;=\; -\frac{\mathrm{Im}D_\alpha(\varepsilon)}{\mathrm{Re}D_\alpha(\varepsilon)} \tag{151}$$

with

$$D_\alpha(\varepsilon) \;=\; \det[1 - G_M(\varepsilon)\;\delta v_{\mathrm{eff}}] \tag{152}$$

Change in the density of states related to phase shift

$$\delta n(\varepsilon) \;=\; \frac{g_\alpha}{\pi}\,\frac{d\delta_\alpha(\varepsilon)}{d\varepsilon} \tag{153}$$

g_α dimension of the representation the state α belongs to

Resonance energy

Let ε_α be the energy where $\mathrm{Re}D_\alpha(\varepsilon)$ vanishes

Taylor expansion: $\mathrm{Re}D_\alpha(\varepsilon) \approx (d\mathrm{Re}D_\alpha(\varepsilon_\alpha)/d\varepsilon)(\varepsilon - \varepsilon_\alpha) \quad \Rightarrow$

$$\tan\delta_\alpha(\varepsilon) \;=\; -\frac{\Gamma}{\varepsilon - \varepsilon_\alpha} \tag{154}$$

with

$$\Gamma \;=\; \left[\frac{\mathrm{Im}D_\alpha(\varepsilon)}{(d\mathrm{Re}D_\alpha(\varepsilon)/d\varepsilon)}\right]_{\varepsilon=\varepsilon_\alpha} \tag{155}$$

$\Rightarrow$ Change in the density of states

$$\delta n(\varepsilon) \;=\; \frac{g_\alpha}{\pi}\,\frac{\Gamma}{(\varepsilon - \varepsilon_a)^2 \;+\; \Gamma^2}\,. \tag{156}$$

Compare with Newns-Anderson expression

Phase shift at the resonance energy

$\Rightarrow$ resonance at energies ε_α where $\mathrm{Re}D_\alpha(\varepsilon)$ vanishes

Phase shift

$$\tan\delta_\alpha(\varepsilon) \;=\; -\frac{\Gamma}{\varepsilon - \varepsilon_\alpha} \tag{157}$$

$\Rightarrow$ phase shift increases through $\pi/2$ as the energy goes through ε_α from below

Lower energy side of the resonance: phase of the reflected wave is shifted such that the electron density is accumulated in the region of the adatom-substrate bond
Bonding character

Higher energy side of the resonance: phase shift leads to a reduction of the the electron density in the region of the adatom-substrate bond
Anti-bonding character

Variation of resonance level

Density of states of H atomic adsorption

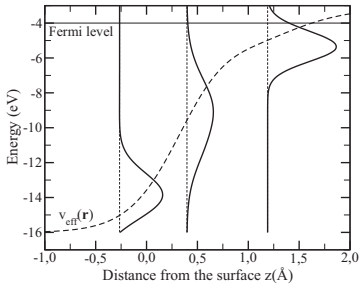

Variation of the density of states as a function of the atomic distance from the surface (Lang and Williams). Electron density corresponds to Al ($r_s = 2$).

Level variation

Resonance levels broadens and shifts to lower energies due to the metal–adatom interaction

Resonance narrows again close to and in the substrate
$\Rightarrow$ Small metal density of states at the bottom of the metal band

Resonance level follows the bare-metal effective potentials
Plausible within first-order perturbation theory

Reactivity concepts for transition and noble metals

Goal: Gain an understanding of the reactivity of a system from properties of the reactand systems alone

Gas-phase reactivity concepts based on the frontier orbital concept (Fukui):

Interaction dominated by the *highest occupied molecular orbital* (HOMO) and the *lowest unoccupied molecular orbital* (LUMO).

Corresponding reactivity concept for reactions at surfaces:

Reactivity determined by metal local density of states at the Fermi energy (Feibelman and Hamann) or by the number of holes in the metal d-band (Harris and Andersson).

Concept of softness (Cohen et al.)

$$s(\vec{r}) \;=\; \left.\frac{\partial n(\varepsilon,\vec{r})}{\partial \mu}\right|_{\varepsilon=\varepsilon_F} \;=\; \int d\vec{r}' \; K^{-1}(\vec{r},\vec{r}')n(\varepsilon_F,\vec{r}) \qquad (158)$$

Hammer and Nørskov: d-band hybridization picture

Adsorption on transition and noble metals

Interaction of atomic level with a transition metal

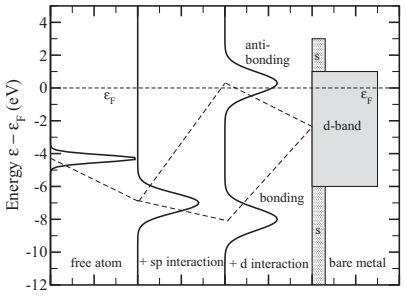

Schematic drawing of the interaction of an atomic level with a transition metal surface

Level variation

Resonance levels broadens and shifts to lower energies due to the sp-metal–adatom interaction
$\Rightarrow$ *Renormalization of energy level*

Renormalized level splits due to the strong hybridization with metal d-states in a bonding and anti-bonding contribution

Up-shift of anti-bonding state larger than down-shift of bonding state
$\Rightarrow$ Overall repulsive effect for complete filling of both the bonding and the anti-bonding resonance

Dissociation of H_2 at metal surfaces

Interaction of molecular levels with a d band metal

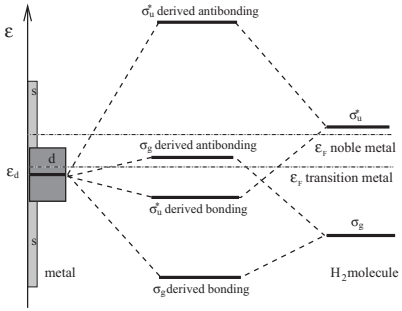

Schematic drawing of the interaction of the H_2 σ_g and σ_u^* levels with a transition metal surface

Interaction

Both σ_g and σ_u^* split into bonding and anti-bonding levels *with respect to the surface–adsorbate* interaction

$\sigma_u^* - d$ interaction attractive since the anti-bonding level is unoccupied

Position of the Fermi energy determines whether the σ_g derived antibonding state is occupied or not

If it is not occupied, the $\sigma_g - d$ interaction is attractive and the H-H bond is weakened due to the occupied σ_u^* level

Approximate reactivity measure in the d-band model

Atomic chemisorption energy

$$\delta E_{\rm chem} \;\approx\; -2(1-f)\,\frac{V^2}{\varepsilon_d - \varepsilon_{\rm H}} \;+\; \alpha V^2 \qquad (159)$$

ε_d center of d-band, $\varepsilon_{\rm H}$ *renormalized* H adsorbate resonance, f filling factor of d-band, first term energy gain due to the hybridization
second term αV^2 repulsion due to energetic cost of orthogonalization

Dissociative adsorption of H_2:
Dissociation barrier determined by the interaction of the renormalized H_2 bonding σ_g **and** the anti-bonding σ_u^* states:

$$\delta E_{ts} \;=\; -2\frac{V^2}{\varepsilon_{\sigma_u^*} - \varepsilon_d} \;-\; 2(1-f)\,\frac{V^2}{\varepsilon_d - \varepsilon_{\sigma_g}} \;+\; \alpha V^2 \qquad (160)$$

Estimate for V: $V = \eta\frac{M_{\rm H}M_d}{r^3}$

Dissociation barriers and d-band model

Correlation between δE_{ts} and E_{ts}^{DFT}

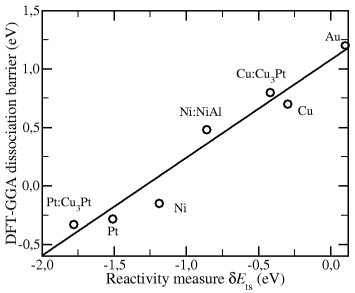

B. Hammer and J.K. Nørskov. Surf. Sci. **343**, 211 (1995).

Discussion

Close correlation between δE_{ts} and E_{ts}^{DFT}

Transition state energies calculated at $(r_{\mathrm{H-H}}, Z) = (1.2\ \text{Å}, 1.5\ \text{Å})$.

Hydrogen dissociates spontaneously on transition metal surfaces.
Noble metals show largest dissocation barriers.

Activation barrier for H_2 dissociative adsorption

Metal	ε_d	V^2	$-2\frac{V^2}{\varepsilon_{\sigma_u^*}-\varepsilon_d}$	$2(1-f)\frac{V^2}{\varepsilon_d-\varepsilon_{\sigma_g}}$	αV^2	δE_{ts}	E_{ts}^{DFT}
Cu	-2.67	2.42	-1.32	0	1.02	-0.30	0.70
Cu:Cu$_3$Pt	-2.35	2.42	-1.44	0	1.02	-0.42	0.80
Pt:Cu$_3$Pt	-2.55	9.44	-5.32	-0.42	3.96	-1.78	-0.33
Pt	-2.75	9.44	-5.03	-0.44	3.96	-1.51	-0.28
Ni	-1.48	2.81	-2.27	-0.10	1.18	-1.19	-0.15
Ni:NiAl	-1.91	2.81	-1.93	-0.11	1.18	-0.86	0.48
Au	-3.91	8.10	-3.30	0	3.40	0.10	1.20

B. Hammer and J.K. Nørskov. Surf. Sci. **343**, 211 (1995). All energies in eV. Transition state energies calculated at $(r_{\mathrm{H-H}}, Z) = (1.2\ \text{Å}, 1.5\ \text{Å})$.

d-band center alone not sufficient to explain reactivity

Hydrogen adsorption on Pd surfaces: a model system for chemisorption

Adsorption of hydrogen on Pd interesting since

- Pd can be used as a catalyst for hydrogenation and dehydrogenation reactions
- Pd can act as a hydrogen storage device ($\rightarrow$ fuel cell technology)

Electronic structure of the free Pd atom:
closed-shell configuration $4d^{10}5s^0$

Open-shell $4d^95s^1$ 0.95 eV higher[1]

Despite the closed-shell configuration of the free atom, Pd shows the reactivity characteristic for a transition metal

H-Pd gas phase chemistry

Pd-H and Pd-H_2 complexes determined on the CASSCF/MRSDCI level

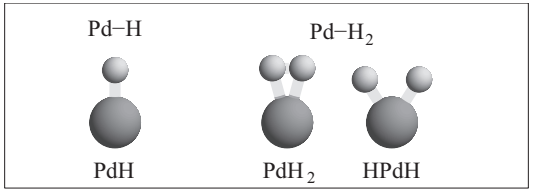

PdH: binding energy $D = 2.34$ eV, bond length $r_e = 1.545$ Å [2]

PdH_2: H-H bond length $r_{\mathrm{H-H}} = 0.864$ Å, Pd-H bond length $r_{\mathrm{Pd-H}} = 1.67$ Å,

HPdH: Pd-H bond length $r_{\mathrm{Pd-H}} = 1.50$ Å, Energy 0.25 eV higher than PdH_2 [3]

PdH_2 weakly bound van der Waals complex, unfortunately no binding energy evaluated

Electronic structure of Pd bulk and surfaces

Local density of states (LDOS)

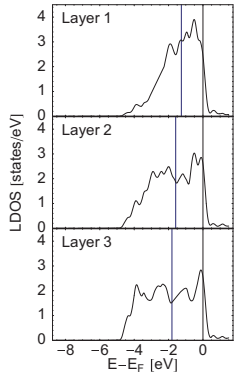

Layer-resolved LDOS of the three topmost layers of Pd(210).

Discussion

Third-layer LDOS already very close to the bulk DOS of Pd

Pd d-band extends over the Fermi energy in the bulk $\Rightarrow$ high reactivity

At the open (210) surface the two upper layers show a significant narrowing and upshift of the d-band

Change of d-band at the surface can be understood within a tight-binding picture

Reactivity model for the description of transition metals

d-band shift due to the lower coordination at surfaces or steps
(B. Hammer *et al.*, Catal. Lett. **43**, 31 (1997), M. Mavrikakis *et al.*, PRL **81**, 2819 (1998).)

$\Rightarrow$ **Higher reactivity**

d-band density of states

Smaller overlap leads to to a narrowing of the d-band

Charge conservation causes a shift of the d-band

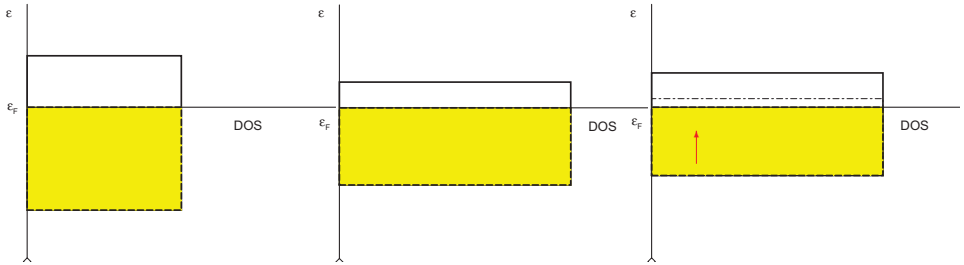

Hydrogen adsorption on Pd(100)

Adsorption energy

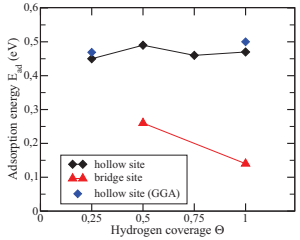

Coverage dependence of the adsorption energy of hydrogen determined by LDA-FP-LMTO calculations (S. Wilke et al., Surf. Sci. **307**, 76 (1994)). GGA calculations: A. Roudgar

Coverage dependence

Coverage dependence can be understood within electrostatic considerations

Adsorption properties for $\Theta = 1$:

Ads. site	E_{ad} (eV)	h_0 (Å)	$\Delta\Phi$ (meV)
hollow	0.47	0.11	180
bridge	0.14	1.01	390

Adsorbate-adsorbate interaction due to dipole-dipole repulsion

Coverage dependence of H adsorption energies on Pd

Adsorption energy per H atom

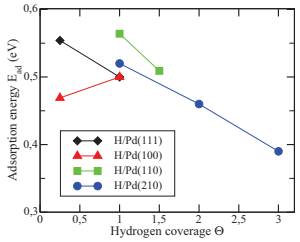

Pd(111) and Pd(100): A. Roudgar
Pd(110): V. Ledentu *et al.*, PRB 57, 12482 (1998)
Pd(210): M. Lischka and A. Groß, PRB 65, Feb. 2002

Coverage dependence

Adsorption energies determined by DFT-GGA calculations with the PW91 exchange-correlation functional

Pd(110): missing-row structure

General trend: H-H interaction repulsive

Reason: repulsive dipole-dipole interaction

Hydrogen adsorption on Pd(110)

H adsorption on unreconstructed Pd(110)

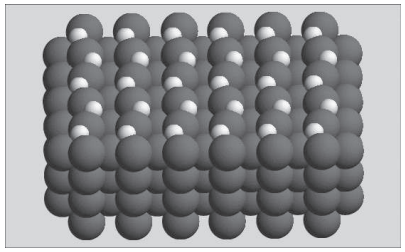

Pd(110): V. Ledentu *et al.*, PRB 57, 12482 (1998)

Adsorption structure

Experiments find a (2×1) structure of H on the unreconstructed Pd(210) surface

GGA-DFT: (2×1) structure 29 meV/H more stable than (1×1) H/Pd(110) structure

Zigzag chains: maximize H-H distance and H screening by the Pd top layer atoms

Both effects reduce dipole-dipole repulsion between adsorbates

Adsorbate-induced reconstructions of Pd(110)

Pairing-row reconstruction

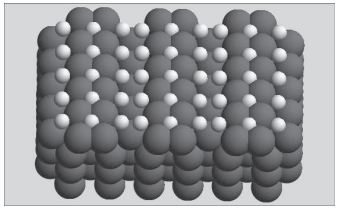

Hydrogen coverage $\Theta = 1.5$

Driving force: H-H repulsion of the adatoms adsorbed in the same trough

Missing-row reconstruction

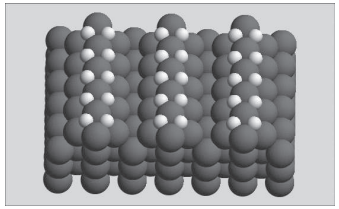

Hydrogen coverage $\Theta = 1.0$

Driving force: better adsorbate-substrate interaction and reduced H-H repulsion

Hydrogen-induced missing-row reconstruction most stable but kinetically hindered

Steps as active centers: H/Pd(210)

Top view of the (210) surface

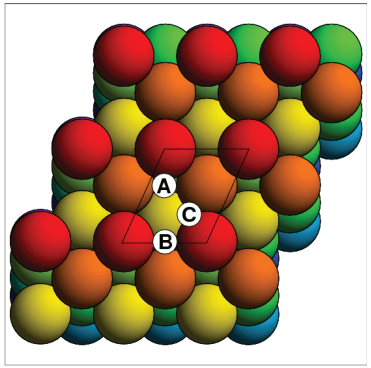

Atomic adsorption energies

Position	Coverage	Theory[1]	Exp.[3]
B	1	0.52	0.41
C	1	0.51	–
A	1	0.45	–
A,B	2	0.40	0.33
A,B,C	3	0.26	0.23
Pd(100)	1	0.50[2]	
Pd(111)	1	0.50[2]	

Adsorption energies for adsorption of an additional H atom

[1]M. Lischka and A. Groß, PRB 65, Feb. 2002; [3]A. Roudgar [3]Muschiol, Schmidt, Christmann, Surf. Sci **395**, 182 (1998)

Preferential adsorption of hydrogen at low-coordinated step sites

Dissociative adsorption of H_2 on Pd(100)

Elbow plots

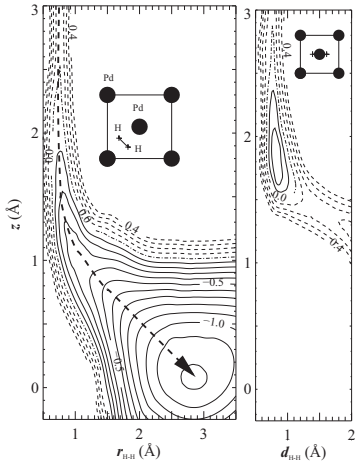

S. Wilke and M. Scheffler, PRB 53, 4926 (1996).

Nonactivated adsorption

On Pd(100), hydrogen dissociates spontaneously along reaction paths without any barrier.

PES depends strongly on the lateral coordinates and the orientation of the hydrogen molecule:

PES highly corrugated and anisotropic

Far away from the surface: H_2 molecule first attracted to the on-top site:

corresponds to dihydride form of PdH_2

In general, chemisorbed molecular states not stable on metal surfaces, H_2 rather dissociates

Coexistence of molecular and atomic adsorption: H/Pd(210)

H_2 molecular chemisorption state stabilized by atomic H adsorption

P.K. Schmidt, K. Christmann, G. Kresse, J. Hafner, M. Lischka, A. Groß, Phys. Rev. Lett. 87, 096103 (2001)

Elbow plot

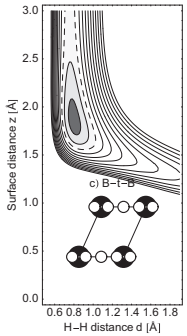

Adsorption properties

state	$E_{ad}(H_2)$ [eV] theor.	exp.
γ_1 ($\theta_H = 1$)	0,29	0,25
γ_2 ($\theta_H = 2$)	0,22	0,16
γ_3 ($\theta_H = 3$)	0,09	–
H_2 vibrational frequency [eV]		
gas phase		0.516
γ_1 ($\theta_H = 1$)	0,42	0,42

Charge density ($\theta_H = 1$)

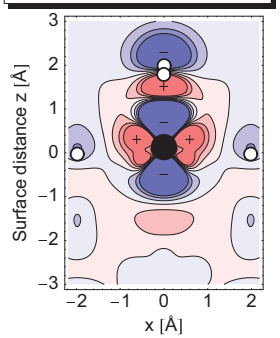

Charge density difference plot

Dissociative adsorption of H_2/Si(100)

On clean Si(100), dissociative adsorption of H_2 activated

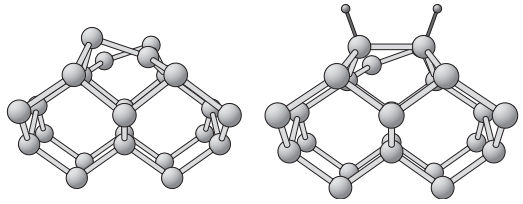

Monohydrid phase: buckling of surface dimers lifted

⇒ Surface rearrangement upon adsorption leads to strong surface temperature effects in the sticking probability

Role of steps in H_2 adsorption on silicon

Hydrogen dissociation on flat Si(100) hindered by sizable energy barrier but on steps spontaneous dissociation possible

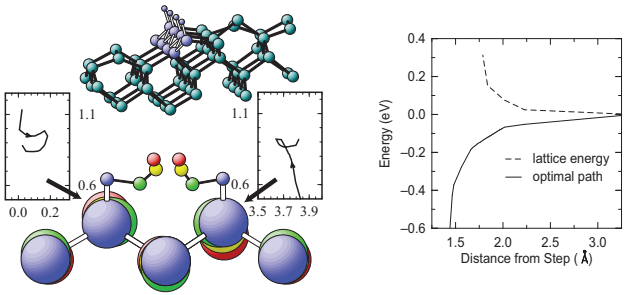

Hydrogen precoverage leads to equivalent electronic properties as on the steps

P. Kratzer et. al, PRL 81, 5596 (1998)

Modification of the surface reactivity by coadsorbates

Coadsorbates can significantly change the surface reactivity

The study of the influence of coadsorbates is – besides of its fundamental interest– of great technological relevance for, e.g., the design of better catalysts

Coadsorbates that enhance the surface reactivity: promoters

Coadsorbates that reduce the surface reactivity: poisoners

Most prominent example for a poison process:
poisoning of the three-way car exhaust catalyst by lead

Sulfur also reduces the performance of car exhaust catalysts

⇒ sulfur-free gasoline will soon be required by law

Poisoning of hydrogen dissociation on Pd

Elbow plots

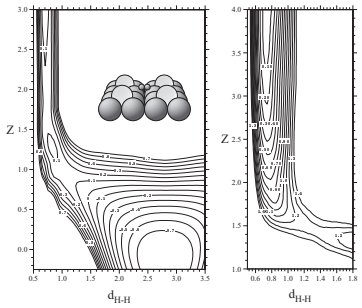

bhb and hth PES of H_2/S(2×2)/Pd(100)
(C.M. Wei, A. Groß and M. Scheffler, PRB 57, 15572 (1998)).

Details of the poisoning

Dissociative adsorption of H_2 still exothermic, but adsorption activated due to the presence of a sulfur (2×2) adlayer

⇒ Sulfur poisoning at low coverages ≤ 0.25 not dominated by site-blocking but by the formation of barriers

Barriers for hydrogen dissociation increase dramatically in the vicinity of sulfur
→ strong repulsion between hydrogen and sulfur

Electronic factors determining the poisoning

Factors: Population of the bonding σ_g and the antibonding σ_u^* molecular states **and** of the bonding and antibonding surface-molecule states

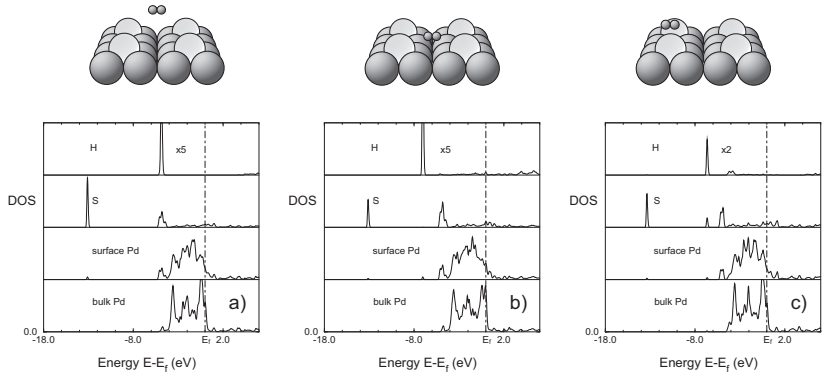

Influence of coadsorption on N_2 adsorption on Ru

Reaction energies

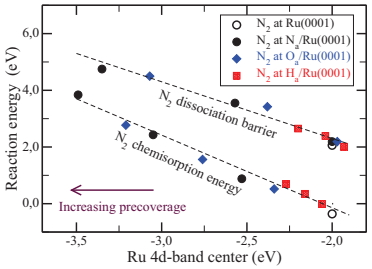

B. Hammer, PRB 63, 205423 (2001).

Coadsorption

Precoverages of N, O and H correspond to 1/4, 1/2 and 3/4 of a monolayer

Coadsorbates N, O, and H shift d-band center to lower energies as a function of the precoverage

d band model: lower d band center correspond to less reactivity

Influence of strain on reactivity

Oxygen-covered strained Ru surface

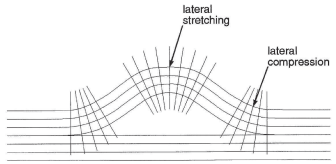

Surface protrusion created by argon implementation

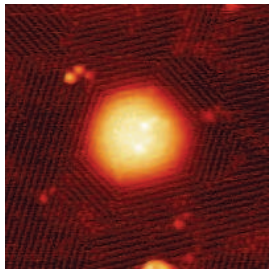

STM image of oxygen adsorption on Ru(0001)
M.Gsell, P.Jakob, and D.Menzel, Science **280**, 717 (1998)

GGA-DFT calculations

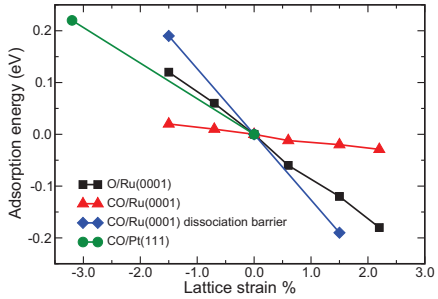

Ru: M. Mavrikakis *et al.*, PRL **81**, 2819 (1998).
Pt: A. Schlapka, M. Lischka *et al.*, PRL **91**, 016101 (2003).

Surface reactivity increases with lattice expansion, as rationalized by the d-band model

Magnitude of reactivity change depends on the particular system: CO/Ru ↔ CO/Pt

Bimetallic surfaces

Bimetallic systems:
Possibility to tailor the reactivity by preparing specific surface compositions and structures

Pseudomorphic overlayer structure

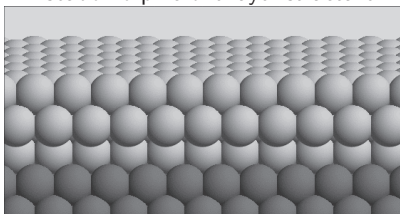

Supported clusters

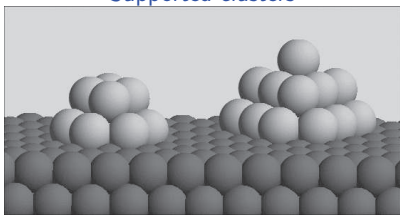

Effects

- Electronic interaction of the overlayers with the substrate
- Geometric strain effects due to lattice mismatch
- Coordination effects
- Cluster-support interaction
- Strain *and relaxation* effects

(see also M.T.M. Koper, Surf. Sci. **548**, 1 (2004))

Alloys not considered here

Simulations allow to disentangle these effects

Pseudomorphic Pt(111) films on Ru(001)

A. Schlapka, M. Lischka, A. Groß, U. Käsberger, and P. Jakob, PRL **91**, 016101 (2003).

STM image (800×800 Å^2)

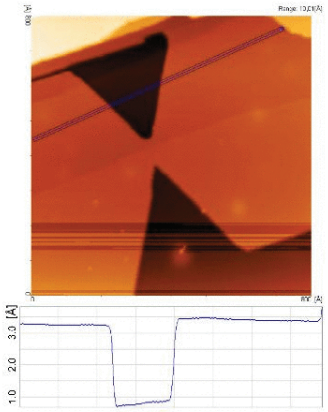

Four monolayers of Pt deposited on Ru(001)
Courtesy of P. Jakob, University of Marburg

Pt/Ru overlayers indeed pseudomorphic

DFT calculations

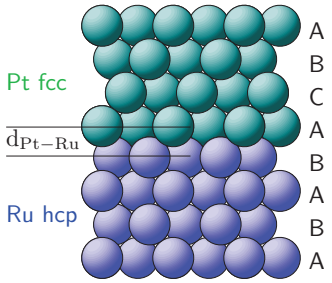

Lattice mismatch Pt/Ru: -2.5%
Stacking: first Pt layer hcp, then fcc
Layer distance: $\Delta d_{Pt-Ru}/d_{Pt-Pt} \approx -7\%$
Cohesive energies:
Ru: 6.74 eV/atom Pt: 5.84 eV/atom

CO adsorption on Pt$_n$/Ru(0001)

A. Schlapka, M. Lischka, A. Groß, U. Käsberger, and P. Jakob, PRL **91**, 016101 (2003).

Measured CO desorption temperatures

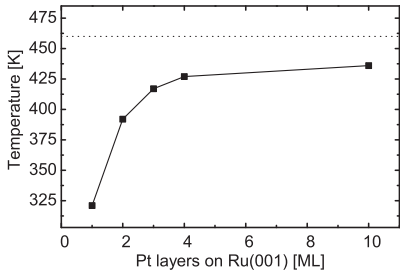

Desorption temperatures of CO from IR spectroscopy and TPD
Dashed line: Pure Pt(111)

Calculated CO adsorption energies

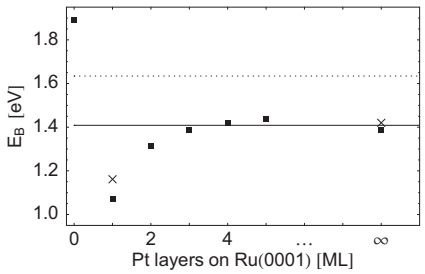

On-top CO binding energies on nPt/Ru(001), for strained Pt (Ru lattice constant) for a $p(2 \times 2)$-CO (solid box) and a $(\sqrt{3} \times \sqrt{3})R30^\circ$ CO overlayer ($\times$)

Similar results for chemisorbed molecular O_2 precursor state

Both strain and substrate interaction effects lead to a reduction in the adsorption energies

CO on Pt$_n$/Ru(001): Comparison with the d band model

A. Schlapka, M. Lischka, A. Groß, U. Käsberger, and P. Jakob, PRL **91**, 016101 (2003).

Correlation with d band center

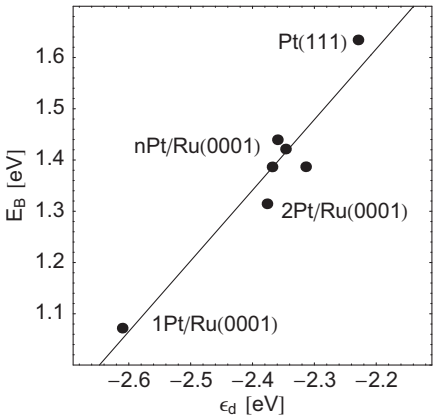

CO adsorption energies as a function of the d band center

Discussion

Pt overlayer on Ru compressed by 2.5 %

Compression leads to increased overlap of d orbitals and downshift of d band center

Strong interlayer bonding between first Pt layer and the Ru substrate layer leads to a further downshift of the d band:

Hypothesis:

Depositing a metal on a more reactive metal makes it less reactive

Substrate-overlayer interaction operative up to the second layer

Good agreement with d band model

Dependence of electrochemical activity on the structure of bimetallic electrodes

Pd/Au structures

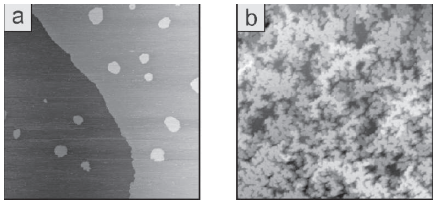

1ML and 5 ML Pd on Au(111) (L.A. Kibler, M. Kleinert, R. Randler, D.M. Kolb, Surf. Sci. 443 (1999) 19)

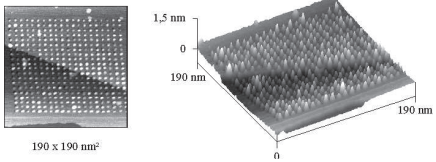

Pd cluster on Au(111) (G.E. Engelmann, J.C. Ziegler, D.M. Kolb, J. Electrochem. Soc. 45 (1998) L 33.)

Discussion

- Electrocatalytic acticivity can depend sensitively on the electrode structure and composition
- Experimentally it is hard to resolve structure ("ensemble") versus composition ("ligand") effects
- Goal: Analyse the electrocatalytic activity of Pd/Au overlayers and clusters by electronic structure methods
- Hydrogen and CO adsorption energies are used as a probe of the electrocatalytic activity
- Unusual electrochemical stability of nanofabricated supported metal clusters

H and CO on Pd_n/Au

A. Roudgar and A. Groß, Phys. Rev. B **67**, 033409 (2003); J. Electroanal. Chem. **548**, 121 (2003).

H/Pd/Au(100) adsorption

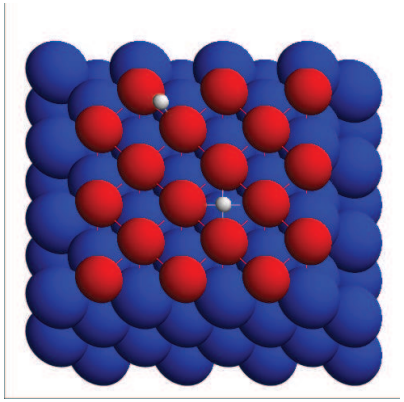

Lattice constants: $a_{\mathrm{Au}} = 4.08$ Å, $a_{\mathrm{Pd}} = 3.89$ Å

$\Rightarrow$ pseudomorphic Pd/Au films expanded by 5%

Bond length effects

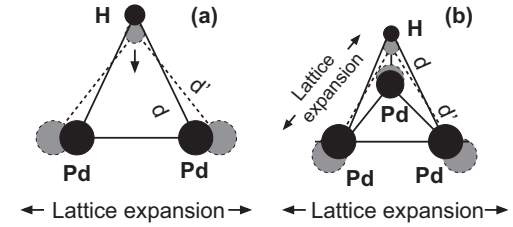

Relaxation of the adsorbate upon lattice expansion

H-Pd distance kept constant with ± 0.01 Å

Exception: fourfold hollow site on $Pd_n/Au(100)$

Adsorption energies of CO and H on Pd_n/Au overlayers

A. Roudgar and A. Groß, Phys. Rev. B **67**, 033409 (2003); J. Electroanal. Chem. **548**, 121 (2003).

$Pd_n/Au(111)$

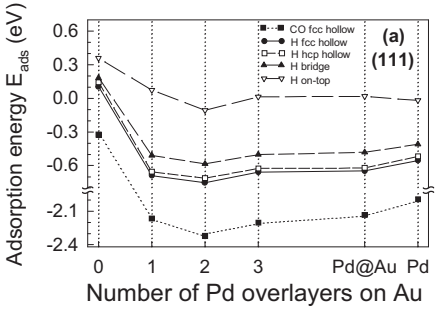

$Pd_n/Au(100)$

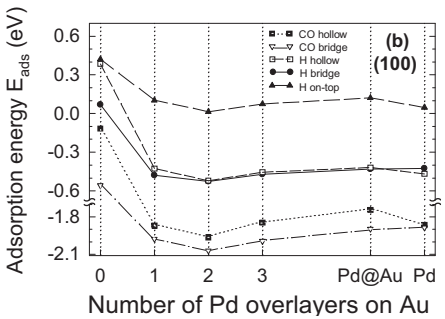

Both strain and substrate interaction effects lead to an increase of the adsorption energies

Maximum of binding energies for both H and CO at all sites on two overlayers

Adsorption on Pd_n/Au overlayers and the d band model

A. Roudgar and A. Groß, Phys. Rev. B **67**, 033409 (2003); J. Electroanal. Chem. **548**, 121 (2003).

d band center

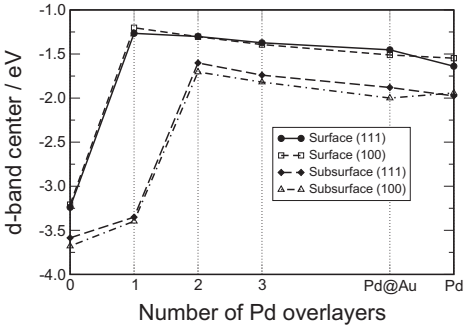

Discussion

Both lattice expansion and overlayer-substrate interaction lead to a upshift of the d band

Expansion of more open Pd(100) surface counterbalanced by inter-layer relaxation effects

Depositing a reactive metal on an inert metal makes it even more reactive

Position of d band centers does not provide an explanation for maximum binding energies on two overlayers

Second layer effects responsible for maximum binding energies on two overlayers

Hydrogen adsorption on PdCu bimetallic surfaces

Pseudomorphic Pd/Cu overlayer compressed by 8%

H/PdCu(111)

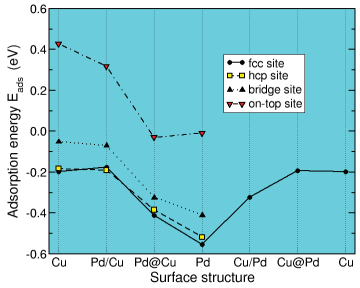

d-band center of surface layer

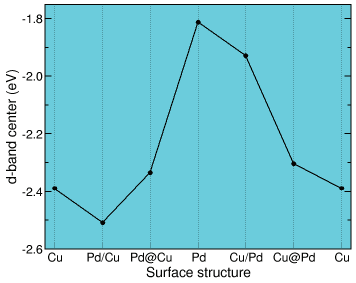

Metallic adsorption energies: Pd/Cu(111): -3.011 eV, Pd/Pd(111): -2.766 eV

PdCu and CuPd overlayer systems show intermediate properties between pure Pd and Cu surfaces due to the strong coupling of Pd and Cu d-electrons

Note: Pd/Cu rather forms surface alloys

(see, e.g., A. Bach Aaen *et al.*, Surf. Sci. **408**, 43 (1998); A. de Siervo *et al.*, Surf. Sci. **504**, 215 (2002))

Pd_n cluster deposited on Au(111)

Pd-Pd distances

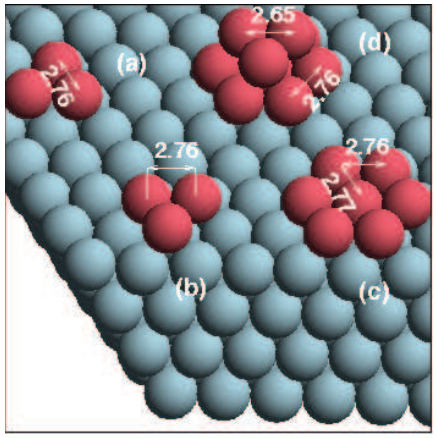

Distances

NN bulk distances:

$d_{Au} = 2.95$ Å, $d_{Pd} = 2.80$ Å

Significant reduction of Pd-Pd distances in supported clusters

Pd-Pd distances in Pd_n/Pd(111) cluster:

Pd_3: 2.69 Å
Pd_7: 2.74 Å

Pd-Pd distances in free Pd_n cluster:

Pd_3: 2.50 Å
Pd_7: 2.64 Å

Electronic structure of Pd_n/Au(111) cluster

Pd_3 Local density of states

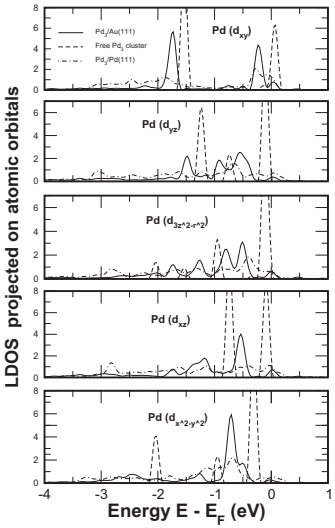

Electronic structure of Pd_3

Pd_3/Au(111): d orbitals confined within the cluster layer (d_{xy} and $d_{x^2-y^2}$) exhibit discrete structure

All other orbitals show a broad spectrum
⇒ strong coupling to the Au substrate

Unusual electrochemical stability of nanofabricated supported metal clusters has been explained by quantum confinement effects

D.M. Kolb *et al.*, Angew. Chemie, Int. Ed. **39**, 1123 (2000)

This speculation is not supported by our calculations

Pd_3/Pd(111): *All* d orbitals broadened
⇒ Even stronger coupling between Pd_3 and Pd(111)

Pd_n cluster deposited on Au(111)

H and CO adsorption energies

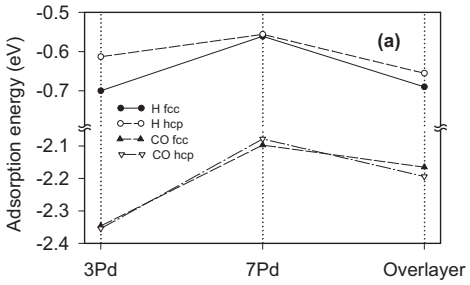

d band positions

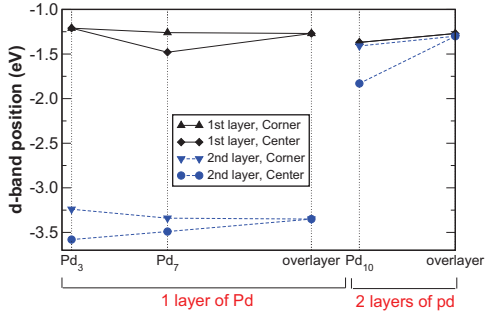

Significant reduction of Pd-Pd distances in supported clusters

Effects of lower coordination in the clusters counterbalanced by compression

H and CO adsorption on Pd_{10}/Au(111) clusters

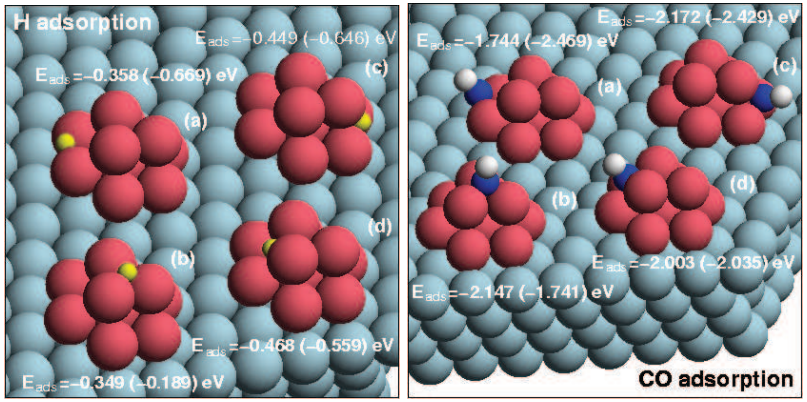

H and CO adsorption energies on Pd_{10}/Au(111) (free Pd_{10}) clusters

Adsorption energies on supported 3D cluster even smaller than on planar clusters

Smaller reactivity of supported 3D cluster due to reduced distances and substrate interaction

Hydrogen evolution on Pd_n/Au(111) clusters

J. Meier, K.A. Friedrich, U. Stimming, Faraday Discuss. **121**, 365 (2002)

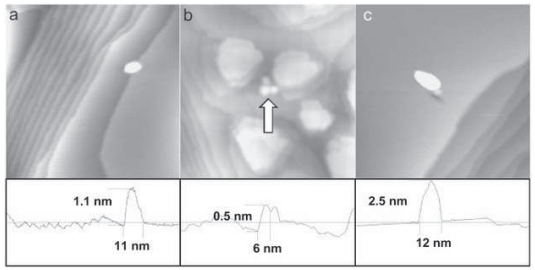

STM images of tip-induced palladium particles on Au

Highest hydrogen evolution rate found for smallest Pd cluster on Au

Kinetic modelling (M. Eikerling,J. Meier, and U. Stimming, Z. Phys. Chem., accept.):

Low hydrogen desorption rate on Pd nanoparticle required
→ Hydrogen spillover to Au substrate from where they are released

Our calculations ⇒ Experiment has probed properties of locally pseudomorphic Pd nano-islands on Au(111) rather than 3D supported nano-clusters

H adsorption in the presence of a water overlayer

Water structures on Pd/Au(111)

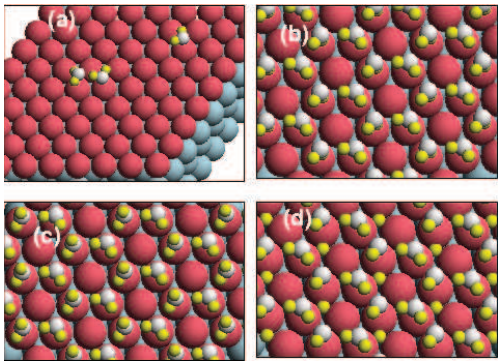

H_2O structure: a) monomer and dimer, b) H-down bilayer (ice Ih), c) H-up bilayer, d) half-dissociated bilayer

H adsorption energies

θ_{H_2O}	$E_{ads}^{H_2O}$	$E_{ads}^{H\,fcc}$	$E_{ads}^{H\,hcp}$
1/4	-0.308	-0.634	-0.592
1/3	-0.295	-0.606	-0.610
1/2	-0.419	-0.582	-0.602
1	+3.135	–	–
3/4	-0.465	-0.561	–
2/3(b)	**-0.528**	**-0.633**	**-0.596**
2/3(c)	-0.499	–	–
2/3(d)	-0.327	–	–
0	–	**-0.690**	**-0.655**

H_2O adsorption energies in eV/H_2O and H adsorption energies ($\theta_H = 1/3$) in eV/atom on Pd/Au(111)

H adsorption energies only slightly changed by the presence of water

(see also S.K. Desai, V. Pallassana, and M. Neurock, J. Phys. Chem. B **105**, 9171 (2001))

CO adsorption in the presence of a water overlayer

CO/water structures on Pd/Au(111)

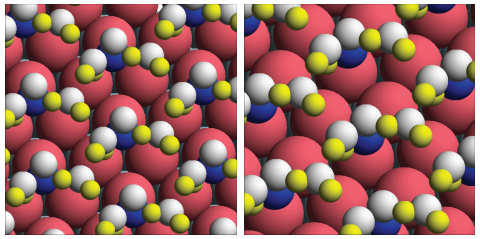

CO/H_2O structures (H-down): a) CO in fcc hollow, b) CO on-top

CO adsorption energies

site	E_{ads}^{CO} H-down	E_{ads}^{CO} H-up	E_{ads}^{CO} clean
fcc	-1.831	-1.894	-2.023
hcp	-1.866	-1.923	-2.043
bridge	—	—	-1.827
on-top	-1.243	—	-1.413

CO adsorption energies ($\theta_{CO} = 1/3$) in eV/molecule on H_2O/Pd/Au(111)

Both H_2O and CO are polar molecules. Still the dipole-dipole interaction between CO and H_2O in the ice-Ih structure on Pd/Au(111) only $\lesssim$ 50 meV

Electric field effect on the H_2O-Pd/Au distance

Water structure under the influence of an external electric field

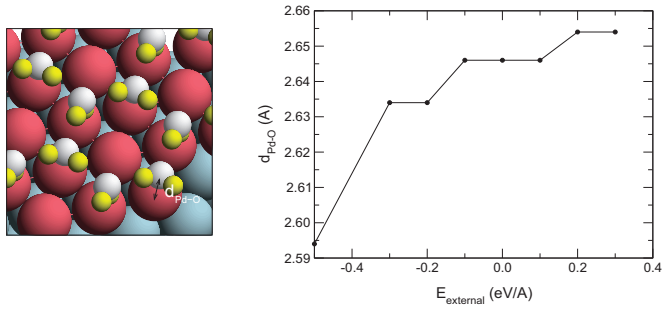

H_2O/Pd/Au structure and H_2O-Pd/Au distance as a function of an external electric field

External electric field introduced via a dipole layer in the vacuum region

Small changes in water-electrode distance for relatively weak electric fields

Water orientation as a function of the electric field

A. Roudgar and A. Groß, Chem. Phys. Lett. **409**, 157 (2005)

Change of the total energy of the H-down and H-up water bilayers as a function of an external electric field

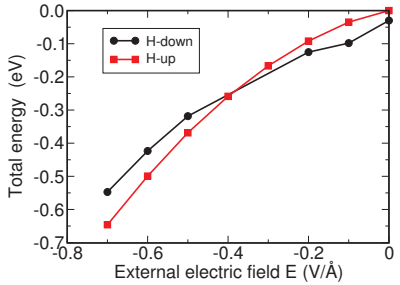

Electric field induces rotation of water bilayer

Field-induced water reorientation confirmed by experiment for H_2O/Ag(111)

K. Morgenstern and R. Nieminen, J. Chem. Phys. **120**, 10786 (2004)

Adsorption at non-zero temperatures and pressures

K. Reuter and M. Scheffler, Appl. Phys. A **78**, 793 (2004)

Heterogeneous catalysis:

Reactions occur under non-zero temperatures and pressures

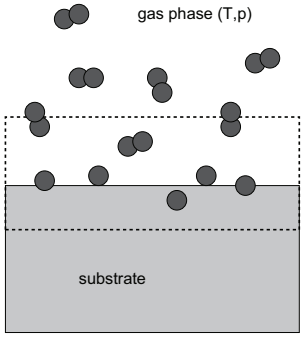

Schematic representation of a substrate in contact with a surrounding gas phase at temperature T and pressure p.

Thermodynamical considerations

Appropriate thermodynamical potential:

Gibbs free energy $G(T, p, N_i)$

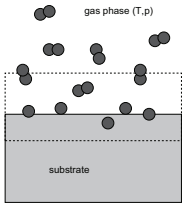

Practical approach: divide whole system in three contributions:

$$G = G_{\text{bulk}} + G_{\text{gas}} + \Delta G_{\text{surface}} . \qquad (161)$$

For bulk and gas, take values for the homogeneous system

Connection between the Gibbs free energy and the total energy calculations:

Helmholtz free energy $F(T, V, N_i)$

$$F(T, V, N_i) = E^{\text{tot}}(V, N) + TS^{\text{conf}} + F^{\text{vib}}(T, V, N_i) , \qquad (162)$$

$$G(T, p, N_i) = F(T, V, N_i) + pV(T, p, N_i) . \qquad (163)$$

Gibbs free energy of adsorption

$N_{\rm M}$ substrate atoms in the surface region per unit cell for the clean surface and $M_{\rm M}$ substrate atoms and $N_{\rm ads}$ adsorbate atoms after adsorption:

Gibbs free energy of adsorption

$$\begin{aligned}\Delta G^{ad}(T,p) &= G(T,p,M_{\rm M},N_{\rm ads}) - G(T,p,N_{\rm M},0) \\ &\quad -(M_{\rm M}-N_{\rm M})\mu_{\rm M}(T,p) - N_{\rm ads}\mu_{\rm gas}(T,p)\ , \end{aligned} \tag{164}$$

$\mu_{\rm M} = g_{\rm bulk}$ and $\mu_{\rm gas} = g_{\rm gas}$:
Gibbs free energies of the substrate and gas atoms, respectively.

Neglect terms from the configurational entropy, the vibrations and the work term pV
(Note that we are concerned with free energy **differences**):

$$\begin{aligned}\Delta G^{ad}(T,p) &\approx E^{\rm tot}(M_{\rm M},N_{\rm ads}) - E^{\rm tot}(N_{\rm M},0) \\ &\quad -(M_{\rm M}-N_{\rm M})E^{\rm tot}_{\rm M} - N_{\rm ads}\mu_{\rm gas}(T,p)\ . \end{aligned} \tag{165}$$

$E^{\rm tot}$: total energy.

Example: Self-assembled Monolayers (SAM)

Self-assembled monolayers of organics molecules on anorganic substrates

Example: Mercaptopyridine on Au(111)

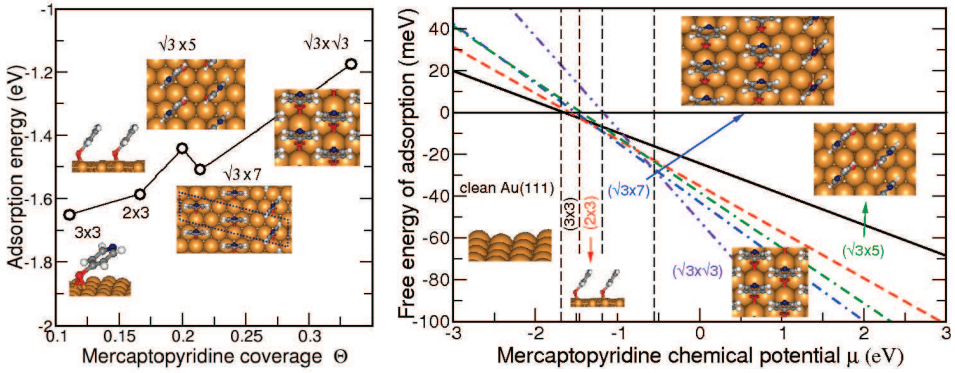

Structure with lowest free energy is stable in a certain range of the chemical potential

J. Kucera and A.Groß, in preparation.

Example: surface oxides

Recently, surface oxide of great interest, in particular in oxidation catalysis

Surface oxides: thin oxide layer on a substrate

Example $(\sqrt{5}\times\sqrt{5})R27^\circ$ PdO surface oxide structure on Pd(100)

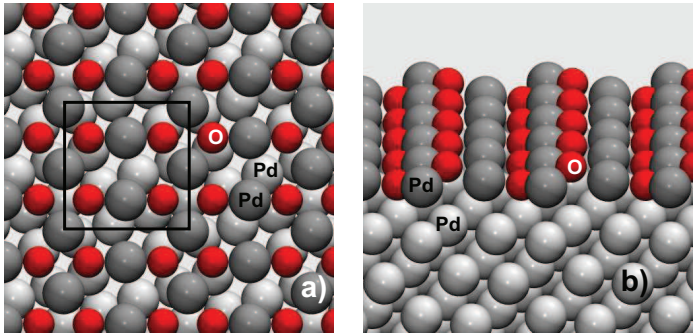

M. Todorova *et al.* Surf. Sci. **541**, 101 (2003).

Chemical potential and adsorption energy

Chemical potential of oxygen:

$$\begin{aligned}\mu_{\rm O}(T,p) &= \frac{1}{2}\mu_{\rm O_2}(T,p) = \frac{1}{2}E^{tot}_{\rm O_2} + \Delta\mu_{\rm O}(T,p) \\ &= \frac{1}{2}E^{tot}_{\rm O_2} + \Delta\mu_{\rm O}(T,p^0) + \frac{1}{2}k_{\rm B}T\ln\left(\frac{p}{p^0}\right)\ . \end{aligned} \tag{166}$$

Definition of the adsorption energy:

$$\begin{aligned}E_{\rm ads} &= \frac{1}{N_{\rm O}}\Big(E^{\rm tot}(M_{\rm M},N_{\rm ads}) - E^{\rm tot}(N_{\rm M},0) \\ &\quad -(M_{\rm M}-N_{\rm M})E^{\rm tot}_{\rm M} - \frac{1}{2}E^{\rm total}_{\rm O_2}\Big)\ , \end{aligned} \tag{167}$$

⇒ **Gibbs free energy of adsorption per surface area** A:

$$\begin{aligned}\Delta\gamma(T,p) &= \gamma(T,p,M_{\rm M},N_{\rm ads}) - \gamma_{\rm clean}(T,p,N_{\rm M},0) \\ &= \frac{1}{A}\Delta G^{ad}(T,p) = \frac{N_{\rm O}}{A}\left(E_{\rm ads} - \Delta\mu_{\rm O}(T,p)\right)\ . \end{aligned} \tag{168}$$

Surface phase diagram of the PdO/Pd(100) system

Free energy of adsorption together with pressure and temperature dependence of the chemical potential:
Surface phase diagram

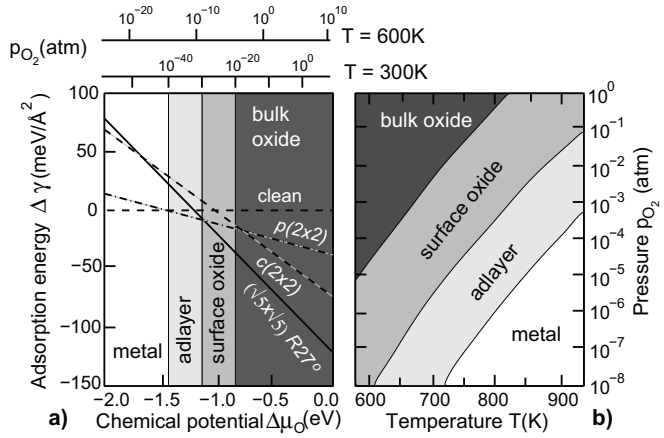

K. Reuter, C. Stampfl, and M. Scheffler, Ab initio atomistic thermodynamics and statistical mechanics of surface properties and functions, in *Handbook of Materials Modeling*, edited by S. Yip, volume 1, page 149, Springer, Berlin, 2005.

Surface phase diagram of the CO+O+Pd(100) system

Surface phase diagrams important to understand structures in heterogeneous catalysis

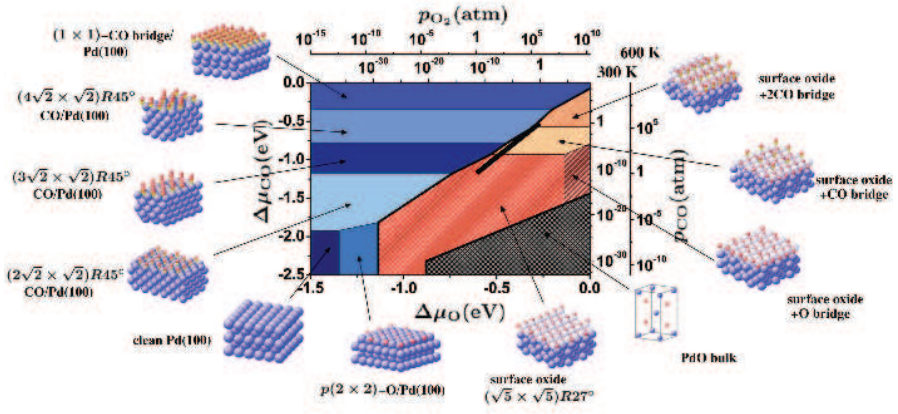

J.Rogal K. Reuter, and M. Scheffler, CO oxidation at Pd(100): A first-principles constrained thermodynamics study, Phys. Rev. B **75**, 205433 (2007).